Differences in neural stem cell identity and differentiation capacity drive divergent regenerative outcomes in lizards and salamanders

Aaron X. Sun[a,b,c], Ricardo Londono[a], Megan L. Hudnall[a], Rocky S. Tuan[a,c], and Thomas P. Lozito[a,1]

[a]Center for Cellular and Molecular Engineering, Department of Orthopaedic Surgery, University of Pittsburgh School of Medicine, Pittsburgh, PA 15219; [b]Medical Scientist Training Program, University of Pittsburgh School of Medicine, Pittsburgh, PA 15213; and [c]Department of Bioengineering, University of Pittsburgh Swanson School of Engineering, Pittsburgh, PA 15213

Edited by Robb Krumlauf, Stowers Institute for Medical Research, Kansas City, MO, and approved July 24, 2018 (received for review March 2, 2018)

While lizards and salamanders both exhibit the ability to regenerate amputated tails, the outcomes achieved by each are markedly different. Salamanders, such as *Ambystoma mexicanum*, regenerate nearly identical copies of original tails. Regenerated lizard tails, however, exhibit important morphological differences compared with originals. Some of these differences concern dorsoventral patterning of regenerated skeletal and spinal cord tissues; regenerated salamander tail tissues exhibit dorsoventral patterning, while regrown lizard tissues do not. Additionally, regenerated lizard tails lack characteristically roof plate-associated structures, such as dorsal root ganglia. We hypothesized that differences in neural stem cells (NSCs) found in the ependyma of regenerated spinal cords account for these divergent regenerative outcomes. Through a combination of immunofluorescent staining, RT-PCR, hedgehog regulation, and transcriptome analysis, we analyzed NSC-dependent tail regeneration. Both salamander and lizard Sox2$^+$ NSCs form neurospheres in culture. While salamander neurospheres exhibit default roof plate identity, lizard neurospheres exhibit default floor plate. Hedgehog signaling regulates dorsalization/ventralization of salamander, but not lizard, NSCs. Examination of NSC differentiation potential in vitro showed that salamander NSCs are capable of neural differentiation into multiple lineages, whereas lizard NSCs are not, which was confirmed by in vivo spinal cord transplantations. Finally, salamander NSCs xenogeneically transplanted into regenerating lizard tail spinal cords were influenced by native lizard NSC hedgehog signals, which favored salamander NSC floor plate differentiation. These findings suggest that NSCs in regenerated lizard and salamander spinal cords are distinct cell populations, and these differences contribute to the vastly different outcomes observed in tail regeneration.

lizard | salamander | neural stem cell | sonic hedgehog | differentiation

Along the evolutionary tree, regenerative capabilities are lost as evolutionary distance to mammals decreases (1, 2). From the ability to fully regrow limbs and organs observed in some species to the fibrotic scarring process observed in many mammalian responses, the healing response is vastly different in both mechanism and outcome (3). To gain insight into these fascinating processes, the axolotl (*Ambystoma mexicanum*) has been extensively studied as a model organism in hopes of elucidating the mechanisms that allow for identical regeneration of many of its tissues (4–13). Our understanding of factors that drive axolotl regenerative potential has grown considerably, but the leap toward affecting regeneration in evolutionarily distant mammals remains a challenge.

Between the axolotl and nonregenerating mammals, lizards sit as an intermediary species on the evolutionary tree and are thought to be the only amniotes capable of tail regeneration (14–16). Lizards possess an "intermediary" ability to regenerate as well, with a peculiar set of morphological differences that distinguish lizard tail regenerates from the originals, unlike the faithfully regenerating salamander tails (14, 17–19). These differences include a striking lack of dorsoventral patterning in the lizard tail regenerate (20), and the key to understanding this unique arrangement of tissues is in identifying the patterning signals involved.

Both lizards and salamanders follow similar mechanisms of tail development during embryonic development. The embryonic spinal cord and surrounding structures are formed and patterned by the neural tube (21, 22). The neural tube exhibits distinct domains: roof plate (characterized by expression of Pax7$^+$, BMP-2$^+$, and Sox10$^+$ among others), lateral domain (Pax6$^+$), and floor plate (Shh$^+$, FoxA2$^+$). The ventral floor plate expresses Shh that, along with the notochord, induces differentiation of surrounding mesoderm into sclerotome, eventually forming the embryonic axial skeleton, while the dorsal roof plate expresses Wnt and BMP that antagonize Shh signaling and induce formation of the dermatome and myotome. These different domains lead to the formation of characteristic roof plate structures, such as sensory dorsal root ganglia (DRG), and floor plate structures, such as motor neurons.

Lizards and salamanders also exhibit similar spinal cord and skeletal development during later stages of development. Dorsal roof plate cells of the neural tube give rise to the sensory interneurons with which neural crest-derived DRG cells synapse, while ventral floor plate cells give rise to motor neurons. During skeletogenesis, sclerotome surrounding the notochord forms vertebrae centrums, neural arches form to enclose tail spinal cords, and hemal arches form around tail arteries. Thus, the general skeletal and central nervous architectures are similar

Significance

The evolutionary changes behind the loss in regenerative potential from salamanders to mammals remain largely elusive. Lizards, representing an intermediary species between the two, possess a limited ability to regenerate their tails. Here, we probe the mechanisms behind the differing regenerative patterns between lizards and salamanders, and we find that neural stem cells within the regenerated spinal cords are distinct cell populations that regulate divergent tail regeneration patterns. This finding sheds light on the factors that govern regenerative ability as well as the loss of this capability and brings us one step closer to eventually elucidating strategies to allow for mammalian regeneration.

Author contributions: A.X.S., R.S.T., and T.P.L. designed research; A.X.S., R.L., M.L.H., and T.P.L. performed research; A.X.S., R.L., M.L.H., and T.P.L. analyzed data; and A.X.S. and T.P.L. wrote the paper.

The authors declare no conflict of interest.

This article is a PNAS Direct Submission.

[1]To whom correspondence should be addressed. Email: tpl9@pitt.edu.

This article contains supporting information online at www.pnas.org/lookup/suppl/doi:10.1073/pnas.1803780115/-/DCSupplemental.

Published online August 13, 2018.

between lizard and salamander tails, which makes the differences in regenerated tissues so surprising.

The regenerated salamander tail spinal cord—specifically the radial glia that line the central canal—has been shown to carry out many of the same roles during tail regeneration as the neural tube during embryonic tail development (7, 23, 24). This ependymal cell population is enriched with neural stem cells (NSCs), and it forms a tube that extends from the original tail stump and infiltrates the regenerating tail blastema. In many ways, this "ependymal tube" is the regenerative analog to the embryonic neural tube. Like the neural tube, the salamander ependymal tube exhibits distinct domains with defined signaling characteristics. In addition to Shh^+ floor plate, $Pax6^+$ and $Pax7^+$ regions demark the lateral plate and roof plate, respectively, and DRGs are reformed (9). Shh produced by the floor plate induces surrounding tail blastema cells to differentiate into cartilage, thereby forming the regenerated salamander tail cartilage rod. The regenerating salamander skeleton follows the same general developmental scheme as during embryonic development. The cartilage rod transitions into vertebrae centrums, and neural and hemal arches form to enclose regenerated tail spinal cords and arteries, respectively. The end result is a regenerated tail skeleton nearly identical to the original. In this way, dorsoventral patterning of the ependymal tube directly influences dorsoventral patterning of other regenerating tissues, including the skeleton.

While lizards also regenerate ependymal tubes and cartilaginous skeletons, they are morphologically simpler, and the end result is very different from the original tails. The regenerated lizard tail skeleton consists of a single unsegmented cartilage tube that completely surrounds the ependymal tube (18). Unlike the salamander cartilage rod, the lizard cartilage tube persists for the lifetime of the regenerate and never transitions into vertebral structures. We have previously shown that the lizard cartilage tube is induced by Shh produced by the ependymal tube, just like the salamander cartilage rod (20, 25). However, unlike the salamander ependymal tube, the lizard ependymal tube does not consist of distinct domains, and DRGs are not reformed. Instead, the entire lizard ependymal tube expresses Shh, effectively designating the entire structure as floor plate. Thus, we hypothesize that the lack of dorsoventral patterning in the regenerated lizard tail is due to dominance of floor plate in the lizard vs. salamander ependymal tube, and the goal of this study is to determine the reasons behind these differences. We report that cells participating in tail regeneration are not homogenous across species, specifically that differences in NSC populations found in the ependyma of spinal cords regenerated by lizards vs. salamanders account, at least in part, for the divergent regenerative outcomes seen in these species with respect to skeletal and central nervous tissues.

Results

Lizards Regenerate Tails with Skeletons and Spinal Cords That Lack Dorsoventral Patterning and Roof-Associated Structures. Both adult lizards and salamanders are able to regrow amputated tails and on gross observation, follow similar time courses in regeneration (*SI Appendix*, Fig. S1). Blastemas form by 14 d postamputation (DPA), and by 28 DPA, regenerated tails are actively elongating. Maturity is reached past 56 DPA, at which point regenerated salamander tails appear similar to originals. Regenerated lizard tails, however, appear noticeably changed in appearance compared with originals, and additional dissimilarities extend to regenerated tissues. Specifically, obvious differences in skeletal and central nervous tissues distinguish regenerated lizard tails from both original lizard and regenerated salamander tails (Fig. 1). Original lizard and salamander tails contain similar vertebral and spinal cord structures as well as similar arrangements (vertebrae centrums ventral to spinal cords) (Fig. 1 *A* and *B* and *SI Appendix*, Fig. S2*A*). However, the regenerated lizard tail skeleton consists of an unsegmented cartilage tube that surrounds the regenerated spinal cord (RSC) (Fig. 1*A′* and *SI Appendix*, Fig. S2*B*), while the regenerated salamander tail exhibits a segmented cartilage rod ventral to the RSC (Fig. 1*B′*). This radial symmetry in regenerated lizard tails is the first indication that dorsoventral patterning is lost during the process of lizard tail regeneration. Similarly, while salamanders and lizards exhibit similar original tail spinal cord morphologies (Fig. 1 *C* and *D* and *SI Appendix*, Fig. S2*A*), another set of striking differences concerns the RSC: the total axonal area in lizard RSCs is greatly reduced (*SI Appendix*, Fig. S2*D* and Table S1), and the characteristic butterfly shape is lost compared with the original (Fig. 1 *C* and *E* and *SI Appendix*, Fig. S2 *A* and *C*). Salamanders, however, regenerate spinal cords that are similar to the originals in both axonal area (*SI Appendix*, Table S1) and shape (Fig. 1 *D* and *G*). In addition, DRG are not regenerated in lizards (Fig. 1*E* and *SI Appendix*, Fig. S2*C*). Instead, regenerated tissues are innervated by extensions of peripheral nerves from DRGs within original tail regions proximal to tail amputation sites (Fig. 1*F*). Unlike lizards, salamanders are able to regenerate DRGs (Fig. 1*G*) (7). Overall, there is a striking lack of roof plate and roof plate-associated structures (i.e., DRGs) within lizard regenerates, which we hypothesize is responsible for many of the differences exhibited by regenerated lizard tails.

Salamanders Regenerate Ependyma with Roof Plate, Floor Plate, and Lateral Domains, While Lizards Regenerate Ependyma with Floor Plate only. Based on observations of the lack of roof plate-associated structures in regenerated lizard tails, we next probed the identity of the lizard ependymal tube. Previous studies have shown that spinal cords and ependymal tubes of original and regenerated salamander tails, respectively, express roof plate, floor plate, and lateral domains (9). As a corollary to this, we investigated the expression patterns of Pax7, Pax6, BMPs, FoxA2, and Shh in original and regenerated lizard tails (Fig. 2). Both original and regenerated salamander spinal cords contained ependyma with distinct $Pax7^+$ BMP-2^+ roof plate, Shh^+ $FoxA2^+$ floor plate, and $Pax6^+$ lateral domains (Fig. 2 *A–H*), while original and regenerated lizard ependyma only expressed floor plate markers Shh and FoxA2 (Fig. 2 *I–P* and *SI Appendix*, Fig. S3 *A–H*). Note that analysis of lizard embryonic neural tubes was included as both validation of lizard antibodies and to emphasize resemblances in marker distributions between the embryonic neural tube and the salamander, but not adult lizard, ependymal tube (Fig. 2 *Q–T* and *SI Appendix*, Fig. S3 *I–L*). Immunofluorescence results were verified by Western blots, which indicated that Pax7 was found to be missing in regenerated lizard but not salamander spinal cords (*SI Appendix*, Fig. S4). Taken together, these results strongly suggest that salamanders, but not lizards, regenerate roof plate ependymal tube domains and more closely recreate the morphology and signaling environment patterned by the neural tube during embryonic development.

Salamander Spinal Cord NSCs Exhibit Roof Plate Identity, While Lizard NSCs Exhibit Floor Plate Identity. Seeking to analyze the sources of patterning molecules within regenerated tails, we turned our attention to the cells within lizard and salamander ependymal tubes. The ependymal tube of the regenerated salamander tail is derived from populations of $Sox2^+$ NSCs found within original tail spinal cord ependyma, and these NSCs form neurospheres in response to FGF stimulation in culture (7). We have identified similar $Sox2^+$ NSCs within the original lizard spinal cord ependyma that also formed neurospheres in culture (Fig. 3 *A–D* and *SI Appendix*, Fig. S5 *A* and *B*). We also analyzed Pax7, Pax6, and Shh expression to determine the positional identity of salamander vs. lizard NSCs in situ and after neurosphere formation in vitro (Fig. 3 *E–P* and *SI Appendix*, Fig. S5 *C–H*). Both salamander and lizard spinal cords contained $Sox2^+$ NSCs. Salamander NSCs were detected in $Pax7^+$ roof plate, $Pax6^+$ lateral domain, and Shh^+ floor plate (Fig. 3 *E–G*), while lizard NSCs

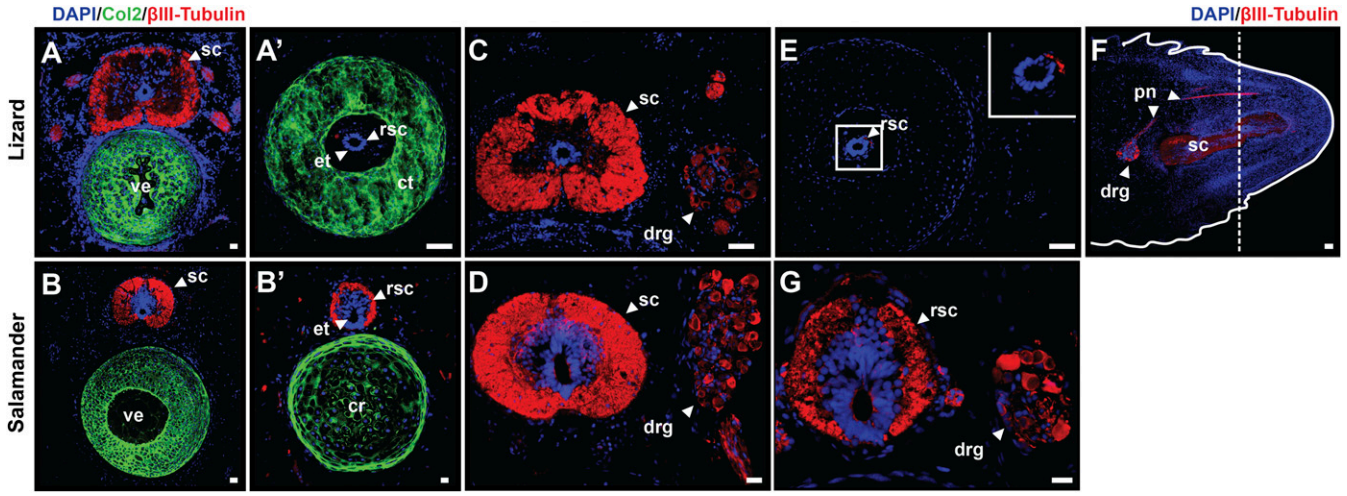

Fig. 1. Salamanders (*A. mexicanum*) regenerate spinal cords with roof plate-associated structures, while lizards (*L. lugubris*) do not. Col2 and βIII-Tubulin immunostaining of original lizard and salamander tail cross-sections (*A* and *B*) and regenerated lizard and salamander tail cross-sections showing cartilage tube in lizards and cartilage rod in salamanders in regenerates, respectively (*A′* and *B′*). (*C* and *D*) βIII-Tubulin immunostaining of original lizard and salamander tail spinal cord cross-sections along with associated DRG. (*E–G*) Immunostaining for βIII-Tubulin in regenerated lizard (*E* and *F*) and salamander (*G*) tails. (Magnification: 2×.) Lizard peripheral nerves are derived from existing nerves proximal to the amputation site (marked with a dashed line), while salamanders regenerate discrete DRG. All regenerates are 8 wk postamputation. cr, Cartilage rod; ct, cartilage tube; drg, DRG; et, ependymal tube; pn, peripheral nerve; rsc, RSC; sc, spinal cord; ve, vertebra. (Scale bar: 50 μm.)

were detected among floor plate only (Fig. 3 *H–J* and *SI Appendix*, Fig. S5 *C–E*). In vitro, both salamander and lizard neurospheres were predominantly Sox2$^+$, indicating high NSC content. Salamander neurospheres were Pax7$^+$ Pax6$^-$ Shh$^-$ (Fig. 3 *K–M*), while lizard neurospheres were Pax7$^-$ Pax6$^-$ Shh$^+$ (Fig. 3 *N–P* and *SI Appendix*, Fig. S5 *F–H*). Western blot analysis verified observed staining patterns (*SI Appendix*, Fig. S4).

Next, we compared lizard and salamander tail spinal cord NSC proliferation both in vivo and in vitro (*SI Appendix*, Figs. S6 and S7); 5-ethynyl-2′-deoxyuridine (EdU) incorporation/staining assays were used to visualize proliferating Sox2$^+$ NSC populations in original and regenerating (14, 28, and 56 DPA) tails along their lengths (proximal, middle, and distal). Salamander Sox2$^+$ NSC populations included more proliferative cells than lizards for all time points and positions, including original tails; 14-DPA samples, which correspond to the blastema stage of regeneration, exhibited the most numbers of proliferative NSCs for both lizards and salamanders. Similarly, 28-DPA samples, which correspond to lengthening tails, exhibited higher numbers of proliferative NSCs than distal regions. Dorsal roof plate-localized Sox2$^+$ cells were more proliferative than ventral floor plate cells in original, proximal 28-DPA, and all 56-DPA salamander samples; no such dorsal/ventral bias was observed in lizards. These in vivo results were mirrored in vitro (*SI Appendix*, Fig. S6). In culture, salamander NSCs, which exhibit roof plate phenotypes, exhibited higher levels of EdU incorporation than lizard NSCs, which exhibit floor plate phenotypes (42.8% for salamanders vs. only 7.9% for lizards). These results suggest a possible roof vs. floor plate dependency on NSC proliferation.

Hedgehog Signaling Regulates Dorsoventral Patterning of Salamander, but Not Lizard, Ependymal Tubes During Tail Regeneration. We next sought to test whether the ependymal tube was responsive to modulation of hedgehog signaling. Previous studies in salamanders found that hedgehog signaling controls both cartilage rod induction and ependymal tube dorsoventral patterning during tail regeneration (9). The lizard cartilage tube is under similar regulation by hedgehog (20), and here, we tested whether these similarities extend to the lizard ependymal tube. The hedgehog inhibitor cyclopamine was administered systemically to both lizards and salamanders ($n = 6$) for 3 wk after tail amputations, and the resulting regenerated tails were analyzed for Pax7 and Shh expression as indicators of ependymal tube dorsoventral patterning and for collagen type II (Col2) expression as a marker for cartilage formation (Fig. 4). As expected, tails regenerated by salamanders treated with vehicle control developed ependymal tubes that expressed Pax7$^+$ roof plate and Shh$^+$ floor plate as well as Col2$^+$ cartilage rods in the ventrum (Fig. 4 *A* and *B*). Lizards treated with vehicle control developed ependymal tubes exhibiting circumferential Shh$^+$ expression and characteristic Col2$^+$ cartilage tubes (Fig. 4 *G* and *H*). Cyclopamine treatment inhibited cartilage formation in both lizards and salamanders as indicated by the loss of Col2 expression in the regenerated tails of both species (Fig. 4 *C* and *I*). In salamanders, cyclopamine also dorsalized ependymal tubes, with marked enhancement of Pax7 expression and reduction of Shh expression (Fig. 4*D*). Like salamanders, cyclopamine treatment inhibited cartilage formation in lizards, with complete disappearance of cartilage tubes (Fig. 4*I*). However, unlike salamanders, lizard ependymal tubes did not respond to cyclopamine treatment. The entire ependymal tube remained positive for Shh expression, and Pax7 levels remained undetectable (Fig. 4*J*). These results suggest that hedgehog signaling in regenerating lizards is not opposed by a dorsalizing signal, which is contrary to salamanders, in which a balance between roof and floor plate signaling exists.

We also tested the effects of the hedgehog agonist Shh agonist (SAG) on regenerated lizard tail ependyma and cartilage patterning. SAG treatment induced sparse ectopic cartilage formation in one of three regenerated salamanders, whereas the response of lizard ectopic cartilage formation to SAG treatment was particularly strong, with extensive cartilage infiltration into various tail regions (three of three samples) (Fig. 4 *E* and *K*). Interestingly, muscle regeneration was also substantially impaired in the SAG-treated animals (*SI Appendix*, Fig. S8). In salamanders, SAG treatment consistently resulted in ventralization of the ependymal tube (Fig. 4*F*). Pax7 expression in dorsal regions was abolished and replaced by Shh, effectively converting the entire ependymal tube into floor plate—similar to the native lizard situation. Again, unlike salamanders, lizard ependymal tubes did not respond to SAG treatment (Fig. 4*L*). Shh expression was maintained by the entire tube, and Pax7 expression

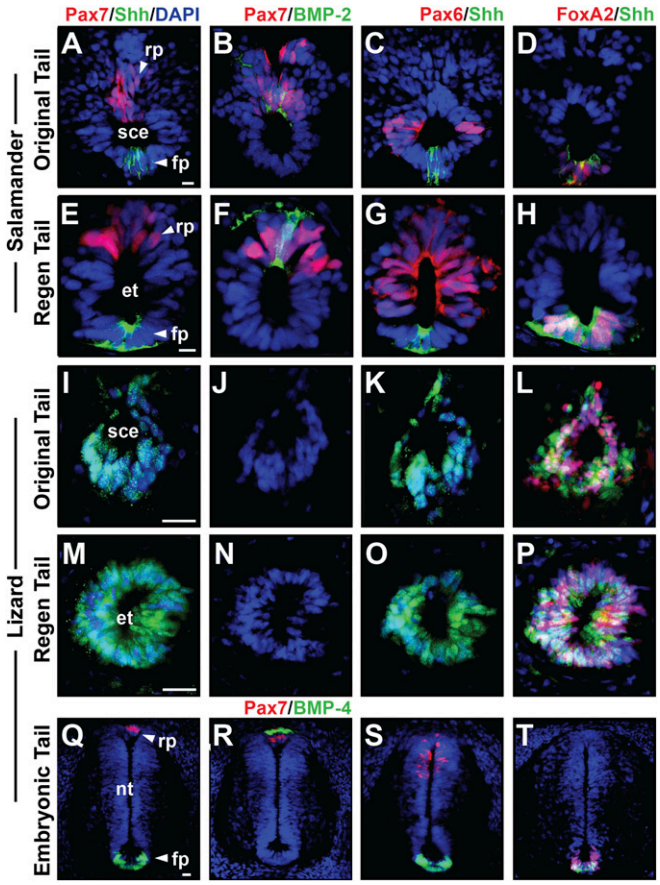

Fig. 2. Salamanders (*A. mexicanum*) regenerate ependymal tubes with roof plate, floor plate, and lateral domains, while lizards (*L. lugubris*) contain floor plate only. Cross-sections of (*A–D*) original salamander tail spinal cord ependyma, (*E–H*) regenerated salamander tail ependymal tubes, (*I–L*) original lizard tail spinal cord ependyma, (*M–P*) regenerated lizard tail ependymal tubes, and (*Q–T*) embryonic lizard tail neural tubes immunostained for roof plate (Pax7, BMP-2/4), lateral plate (Pax6), and floor plate (FoxA2, Shh) markers. Original and regenerated salamander ependymal tubes exhibit roof, lateral, and floor plate domains, while original and regenerated lizard ependymal tubes only contain floor plate. The embryonic lizard tail neural tube, however, also contains all three domains. All regenerates are 8 wk postamputation. et, Ependymal tube; fp, floor plate; nt, neural tube; rp, roof plate; sce, spinal cord ependyma. (Scale bar: 50 μm; scale in *A*, *E*, *I*, *M*, and *Q* also applies to *B–D*, *F–H*, *J–L*, *N–P*, and *R–T*, respectively.)

remained undetectable. Taken together, these results suggest that hedgehog signaling regulates dorsoventral patterning in the salamander, but not lizard, ependymal tube. The striking differences in responsiveness between lizard cartilage and ependymal cells to exogenous hedgehog inhibition and stimulation are particularly interesting. The strong responsiveness of lizard cartilage to both SAG and cyclopamine treatments indicated effective treatment methods on lizard regenerated tails, and yet, no changes in ependymal tube dorsoventral patterning were observed compared with vehicle controls. This is in direct contrast to dorsoventral patterning of the salamander ependymal tube, which was strongly influenced by hedgehog signaling. These results offer evidence of the pervasive and persistent properties of lizard NSC floor plate identity.

We next investigated the same signaling pathways in vitro, asking how these populations responded to hedgehog signaling when removed from the regenerating tail environment (Fig. 5 and *SI Appendix*, Fig. S9). Default roof plate salamander neurospheres were unaffected by cyclopamine treatment and maintained high levels of Pax7 and undetectable Shh expression levels (Fig. 5*B*). In contrast, administration of SAG resulted in the replacement of Pax7 with Shh expression (Fig. 5*C*). These results correlate well with the in vivo findings, where a fine balance exists between salamander ependymal tube roof and floor plate signaling, and stimulation of hedgehog signaling expands floor plate at the expense of roof plate. However, lizard neurospheres seemed to follow a different model. Cyclopamine administration did not abolish Shh, and SAG signaling did not cause an appreciable difference by immunostaining (Fig. 5 *D–F* and *SI Appendix*, Fig. S9). Immunostaining results were verified by Western blots (Fig. 5 *G* and *H*) and corroborated by real time RT-PCR gene expression analysis, in which a significant decrease in Shh expression was observed with SAG administration along with a small increase in Shh on cyclopamine treatment (*SI Appendix*, Fig. S10). These results point to a model where Shh is constitutively expressed by lizard NSCs, and a negative feedback mechanism exists to control Shh gene levels. Notably, Pax7 levels were at the limit of detection or undetectable in all cohorts of lizard NSCs. Taken together, the in vivo and in vitro results from our experiments in Figs. 4 and 5 and *SI Appendix*, Figs. S9 and S10 suggest that lizard NSCs are distinctly different compared with salamander NSCs in the way that they work to pattern the regenerating tail.

Fig. 6 summarizes our hypothesis on the differences between salamander and lizard NSC populations. Salamander NSCs are found in all domains (roof, lateral, and floor) within the original tail spinal cord. In the absence of hedgehog signaling, salamander NSCs exhibit roof plate markers and are subsequently ventralized by Shh signaling to create the roof, lateral, and floor plate domains observed in the regenerated ependymal tube. NSCs isolated from the original adult lizard spinal cord ependyma (expressing only floor plate) maintain their default floor plate signaling, even in the absence of hedgehog signaling. Lizard NSCs are unable to dorsalize, and their inherent floor plate identity is propagated into the regenerated tail.

Unlike Salamanders, Lizards Do Not Regenerate New Spinal Cord Neurons. Given the disparities in lizard vs. salamander NSC positional identities and the markedly decreased axonal staining levels in lizard tail regenerates, we next compared the differentiation capacities of salamander and lizard NSCs into multiple neural lineages. We first showed differences in differentiation capacities in vivo. Salamander and lizard spinal cords were transplanted into regenerating tails to observe the differentiation capabilities of transferred NSCs. As expected, original salamander spinal cords proximal to amputation sites exhibited Sox2, β-tubulin, and glial fibrillary acidic protein (GFAP) staining (Fig. 7*A*), while regenerated salamander spinal cords also exhibited these lineages (Fig. 7*B*)—indicating reconstitution of multiple neural lineages. Implanted salamander spinals cord proximal to the amputation site contained no β-tubulin staining (Fig. 7*E*)—as one would expect due to loss of innervation of the neurons—but the regenerated cord again displayed the full range of neural lineages (Fig. 7*F*). These results suggest that even standalone populations of regenerating and differentiating salamander NSCs are capable of reconstituting multiple neural lineages. These results differ drastically from those observed with lizard NSCs. Original lizard spinal cords proximal to amputation planes exhibited robust β-tubulin and GFAP staining (Fig. 7*C*), while regenerated lizard spinal cords showed only spotty axon staining (Fig. 7*D*). Interestingly, implanted spinal cords, whether they were proximal or distal to the amputation site, did not exhibit any neural staining, except for GFAP (Fig. 7 *G* and *H*). These results suggest that the NSC populations within the lizard spinal cord do not have the ability to reconstitute multiple lineages (only GFAP$^+$ astrocytic lineages) and that axons in the regenerate likely arise from extension of axons proximal to the amputation site rather than NSC differentiation.

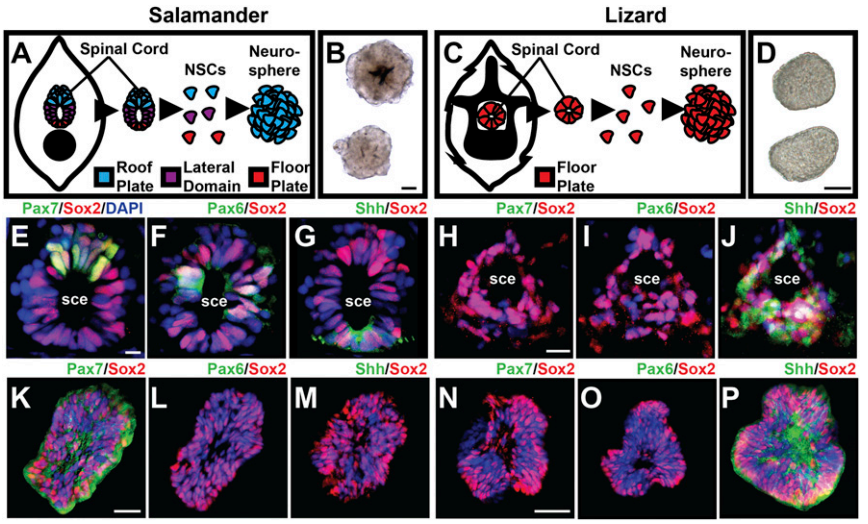

Fig. 3. Salamander (*A. mexicanum*) NSCs exhibit roof plate identity, while lizard (*L. lugubris*) NSCs exhibit floor plate identity. (*A–D*) Summary schematic of NSC neurosphere formation: salamanders default to roof plate, and lizards default to floor plate. (*B* and *D*) Light microscopy of neurospheres formed in vitro for salamanders and lizards, respectively. (*E–G*) Roof (Pax7), lateral (Pax6), and floor (Shh) plate immunostaining of Sox2$^+$ NSCs in salamander tail spinal cord ependyma. (*H–J*) Roof, lateral, and floor plate staining of Sox2$^+$ NSCs in lizard spinal cord ependyma. (*K–M*) Roof, lateral, and floor plate staining of in vitro cultured salamander neurospheres. Note the absence of lateral and floor plate markers. (*N–P*) Roof, lateral, and floor plate staining of in vitro cultured lizard neurospheres. Note the absence of lateral and roof plate markers. Neurospheres were isolated from original tails. sce, spinal cord ependyma. (Scale bar: 50 μm; scale in *E*, *H*, *K*, and *N* also applies to *F* and *G*, *I* and *J*, *L* and *M*, and *O* and *P*, respectively.)

Again, to probe the behavior of these NSCs outside the regenerative environment, we cultured salamander and lizard neurospheres and subsequently exposed them to differentiation conditions to test their differentiation potential in vitro. Strikingly, differentiated salamander neurospheres were positive for β-tubulin (neuron marker) and GFAP (astrocyte marker) (26), while differentiated lizard neurospheres only expressed GFAP (Fig. 8 and *SI Appendix*, Fig. S11). In addition, we verified the differentiation behavior of lizard NSCs through real time RT-PCR and found that only GFAP was significantly up-regulated, with concomitant down-regulation of NSC marker Sox2 and lineage markers neurofilament heavy (neuronal lineage) and Sox10 (oligodendrocyte) (*SI Appendix*, Fig. S12). The ability of salamander neurospheres to differentiate into multiple lineages is consistent with observations by Mchedlishvili et al. (7), who described the ability of salamander NSCs to reconstitute both the CNS and the peripheral nervous system. Our findings, however, suggest that lizard NSCs are lineage restricted in their differentiation capacity. These results correlate well with our in vivo observations that exogenous spinal cord implants harboring Sox2$^+$ ependymal cells are not able to reform a spinal cord within the regenerated tail—they only express GFAP just as they do during in vitro differentiation. Overall, we see not only that lizard NSCs are restricted to floor plate domains but that they are also restricted to GFAP$^+$ neural lineages—a complete divergence from the versatile salamander NSCs.

Salamander NSCs Are Ventralized Within the Lizard Tail Microenvironment by Hedgehog Signaling. With the finding that lizard NSCs were restricted in lineage potential and patterning identity, we asked if the introduction of Pax7$^+$ salamander NSCs would be sufficient to induce a different regenerative response in the regenerating lizard ependymal tube. Of note, we also tried the reverse experiments with lizard NSCs injected into salamander tails but found that they did not survive the aquatic environment. We first verified that isolated lizard NSCs were in fact able to reconstitute the regenerating ependymal tube in vivo (*SI Appendix*, Fig. S13). NSCs prelabeled with the membrane dye 1,1′-Dioctadecyl-3,3,3′,3′-tetramethylindocarbocyanine perchlorate (DiI) were injected into

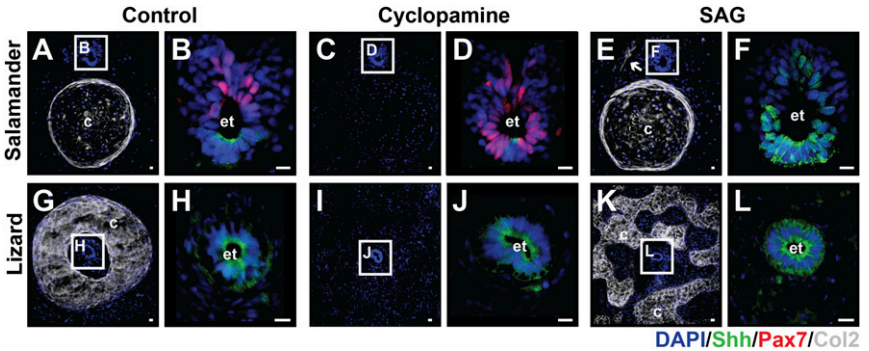

Fig. 4. Hedgehog signaling is necessary for the correct establishment of dorsal ventral progenitor domains in the ependymal tube during tail regeneration. Pax7, Shh, and Col2 staining of control regenerated tails (*A*, *B*, *G*, and *H*), cyclopamine-treated regenerated tails (*C*, *D*, *I*, and *J*), and SAG-treated regenerated tails (*E*, *F*, *K*, and *L*) in salamanders (*A. mexicanum*; *A–F*) and lizards (*L. lugubris*; *G–L*), respectively. Ependymal tubes enclosed in white boxes are shown in magnified view to the right of the corresponding image. All regenerates are 4 wk postamputation. c, Cartilage; et, ependymal tube. (Scale bar: 50 μm.)

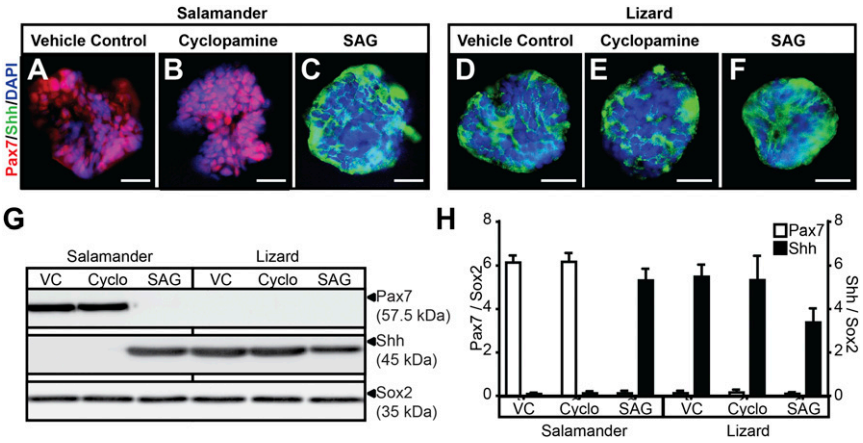

Fig. 5. Ventralization of salamander (*A. mexicanum*), but not lizard (*L. lugubris*), neurospheres is regulated by hedgehog signaling. (*A–C*) Roof (Pax7) and floor plate (Shh) staining of in vitro salamander neurospheres treated with control, cyclopamine, and SAG. Pax7 and Shh expression is responsive to SAG treatment. (*D–F*) Roof (Pax7) and floor plate (Shh) staining of in vitro lizard neurospheres treated with control, cyclopamine, and SAG. Shh expression is unaffected by treatments. (*G*) Western blot analysis of Pax7, Shh, and Sox2 in salamander and lizard neurospheres treated with vehicle control (VC), cyclopamine (Cyclo), and SAG. (*H*) Quantification of Western blot intensities. Neurospheres were isolated from original tails ($n = 3$). (Scale bar: 50 μm.)

original spinal cord ependyma of amputated lizard tails. After 28 d, regenerated tail ependymal tubes were assayed for colocalization on DiI and Sox2 expression. DiI$^+$ Sox2$^+$ cells were found throughout the ependymal tubes of regenerated tails. These results showed incorporation of injected NSCs into regenerated lizard tail spinal cords.

Next, we sought to induce a different patterning identity in the regenerating lizard ependymal tube through the introduction of Pax7$^+$ salamander NSCs. To avoid rejection of xenogeneic cells and to test for the role of hedgehog signaling in cell fate, we opted to inject DiI-labeled, in vitro-cultured NSCs into the spinal cords of amputated lizard tails treated with the immunosuppressant Tacrolimus with or without cyclopamine treatment (*SI Appendix*, Fig. S14). As controls, lizard NSCs were also injected under the same conditions. After tail regeneration, DiI-labeled salamander cells were found to have been ventralized within the regenerating ependymal tube (Fig. 9*A*). However, when Shh signaling was inhibited with cyclopamine, the xenogeneic salamander NSCs retained Pax7 positivity, and Shh expression was spatially limited, reminiscent of embryonic dorsal–ventral patterning (Fig. 9*B*). As controls, lizard NSCs were also injected into separate animals and subjected to the same treatments (Fig. 9 *C* and *D*). As expected, regardless of the microenvironment, the lizard NSCs remained Shh$^+$. These results taken together indicate that the native microenvironment created by regenerated lizard spinal cord NSCs is nonconducive to roof plate differentiation given its strong ventralizing Shh expression.

Salamander NSCs Differentiate into Neural Lineages Within the Lizard Microenvironment. Lastly, we tested the ability of salamander NSCs to differentiate into neurons within the microenvironment of the regenerating lizard tail (Fig. 10). Salamander NSCs were expanded in vitro, labeled with DiI, and injected into amputated lizard tails during treatment with Tacrolimus. Regenerated tails were then assayed for differentiation of DiI-labeled cells intro neuronal and astrocyte lineages. As controls, lizard NSCs were injected under the same conditions into lizard tails, and salamander NSCs were also injected back into salamander tails to verify their functionality in the microenvironment of the regenerating salamander tail. Note that the condition involving injection of DiI-labeled lizard cells into salamander tails was attempted, but lizard cells did not survive within salamanders and were not detected in regenerate salamander tails. As expected based on findings by Mchedlishvili et al. (7), DiI-labeled salamander NSCs injected into salamander tails were able to differentiate into neurons (evidenced by βIII-Tubulin/DiI colocalization) and astrocytes (GFAP/DiI colocalization) (Fig. 10 *A* and *B*). Interestingly, DiI-labeled salamander NSCs injected into lizard tails retained their abilities to differentiate into

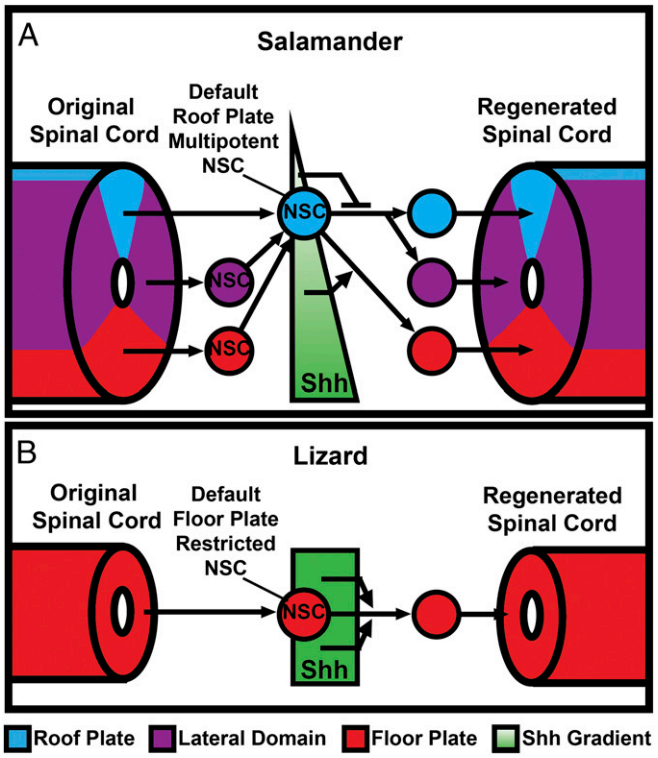

Fig. 6. Hypothesized patterning signals found in salamander and lizard NSCs. (*A*) The ependyma of the original salamander tails harbors NSCs that contain organized roof, lateral, and floor plate domains, which are default roof plate within their environment and on explant and culture in vitro. They are responsive to hedgehog signaling and ventralize according to a hedgehog gradient, and in this fashion, they drive regeneration and patterning in the salamander tail regenerate. (*B*) The lizard original tail ependyma is composed of solely floor plate NSCs, which remain floor plate on explant and culture in vitro. They remain floor plate regardless of perturbations in hedgehog signaling and pattern the regenerated lizard tail as such.

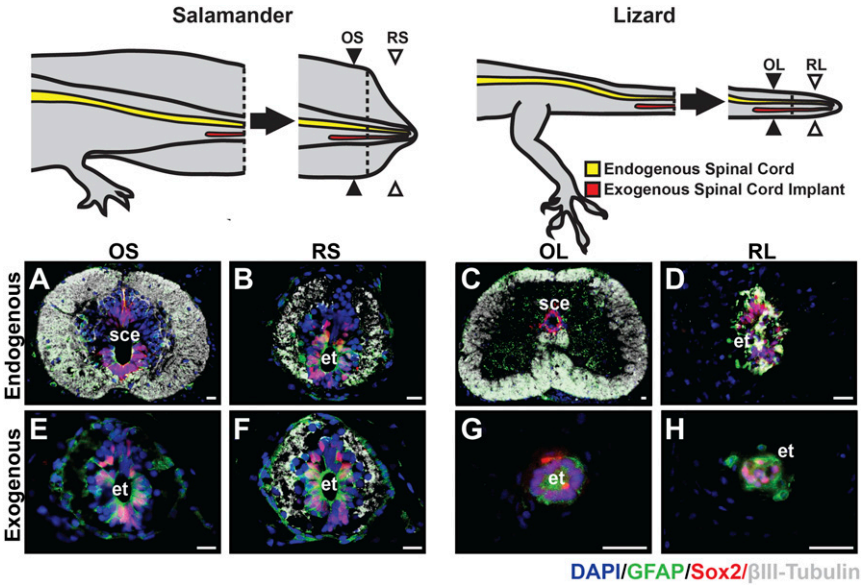

Fig. 7. Salamanders (*A. mexicanum*) regenerate new neurons during tail regeneration, while lizards (*A. carolinensis*) do not. Exogenous spinal cords were allogeneically implanted into salamander and lizard tails followed by reamputation. βIII-Tubulin, GFAP, and Sox2 staining of spinal cords proximal to amputation site (*A* and *C*/*E* and *G*) and distal to amputation site (*B* and *D*/*F* and *H*) in the endogenous/exogenous spinal cords of the salamander and lizard tail, respectively. Exogenous spinal cords in the salamander are able to reconstitute multiple neural lineages, whereas in lizards, they cannot. All regenerates are 4 wk postamputation. et, Ependymal tube; OL, original lizard spinal cord; OS, original salamander spinal cord; RL, regenerated lizard spinal cord; RS, regenerated salamander spinal cord; sce, spinal cord ependyma. (Scale bar: 50 μm.)

both neurons and astrocytes (DRGs were not observed) (Fig. 10 *C* and *D*). In contrast, DiI-labeled lizard NSCs injected into lizard tails expressed only GFAP, with characteristic absence of β-tubulin (Fig. 10 *E* and *F*). Instead, we observed sparse β-tubulin$^+$ DiI$^-$ axons running within the RSC, presumably derived from extensions of the axons proximal to the amputation site (Fig. 10*E*). These results suggest that lizard Sox2$^+$ GFAP$^+$ NSCs only contribute to the Sox2$^+$ GFAP$^+$ cells of the ependymal tube, and based on our observations, they are not found in any other neural structure, again indicating a restriction in neural differentiation capacity compared with salamander NSCs.

The effects of the regenerated lizard and salamander tail microenvironments on differentiation of DiI-labeled salamander NSCs into roof and floor plate lineages were also tested (*SI Appendix*, Fig. S15). Salamander NSCs injected into salamander tails contributed to both Pax7$^+$ roof plate and Shh$^+$ floor plate domains (*SI Appendix*, Fig. S15*A*). In contrast, both salamander and lizard NSCs injected into lizard tails exhibited Shh expression and no indication of Pax7 expression (*SI Appendix*, Fig. S15 *B* and *C*). Overall, these results indicate that salamander NSCs retain their ability to differentiate into neurons, despite taking on floor plate identity within the ventralizing regenerated lizard tail microenvironment, and they suggest that the inability of lizard NSCs to differentiate into neural linages is a property inherent to lizard NSCs and is not a product of the lizard tail microenvironment.

Discussion

In this study, we examined the role of Sox2$^+$ NSCs in driving divergent tail regeneration outcomes in lizards vs. salamanders. These NSCs are critical to regeneration, as newly RSC cells are wholly derived from NSCs in both lizards and salamanders. The first clues that phenotypic differences exhibited by the regenerated lizard tails were linked to deficiencies in NSC populations were based on observations that salamanders regenerate roof plate structures (in particular, sensory neurons), while lizards do not. Additional investigation revealed that salamander and lizard NSCs are distinct populations of cells with differing regional identities and differentiation capabilities. NSC hedgehog signaling is responsible and necessary for correct establishment of dorsoventral progenitor domains within the regenerating ependymal tube of salamanders. In addition, the Shh signals produced

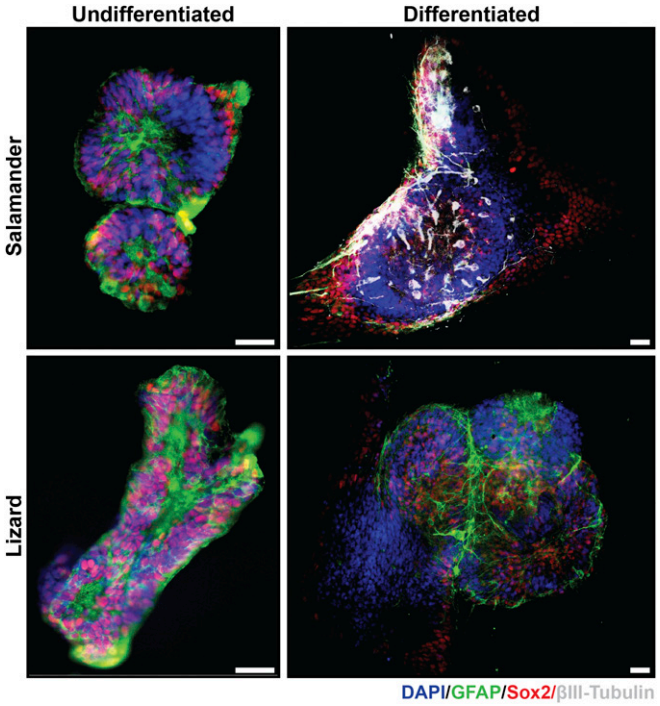

Fig. 8. Salamander (*A. mexicanum*) NSCs are capable of neuronal differentiation into neurons, whereas lizard (*L. lugubris*) NSCs are not. βIII-Tubulin, GFAP, and Sox2 staining of differentiated and undifferentiated salamander and lizard neurospheres. Note the inability to form axons. (Scale bar: 50 μm.)

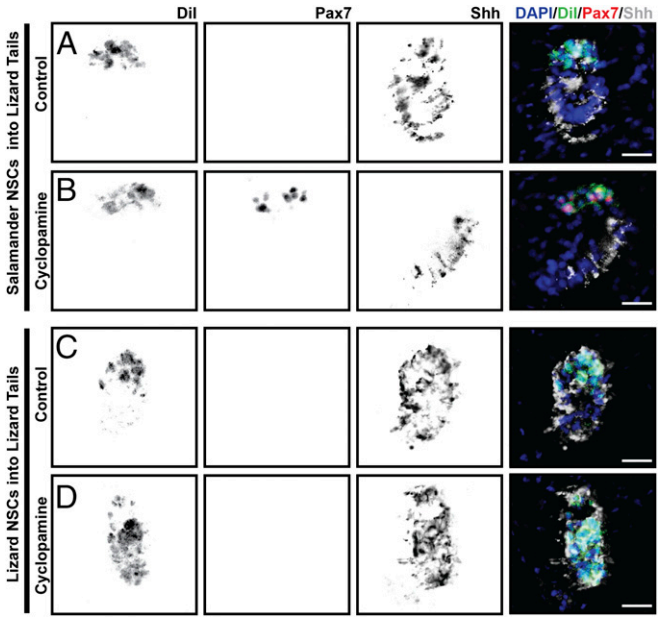

Fig. 9. Salamander (*A. mexicanum*) NSCs are ventralized within the lizard (*L. lugubris*) tail microenvironment. Salamander and lizard neurospheres were cultured in vitro, DiI labeled, and injected into the spinal cord of an amputated lizard tail. (*A–D*) Transverse sections of the regenerated ependymal tube stained for roof plate marker Pax7 and floor plate marker Shh with or without cyclopamine treatment for the lizards. Note the Pax7 negativity of salamander NSCs in noncyclopamine-treated lizards vs. the corresponding Pax7 positivity and patterning segregation in cyclopamine-treated lizards. All regenerates are 2 wk postamputation/NSC injection. (Scale bar: 50 μm.)

by both the salamander and lizard ependymal tubes are responsible for patterning the axial skeletons in the regenerated tails of both these species, similar to the induction and patterning of the axial skeleton by the embryonic neural tube during development (9, 20–22, 25). Here, we show that the floor plate-restricted differential potential of lizard NSCs results in lack of dorsoventral patterning and roof plate structures within the lizard regenerate. Thus, the disparities between both the regenerated lizard CNS and skeletal system compared with those of regenerated salamander tails can be linked to distinct differences in NSC populations.

Salamanders and lizards present distinct models of regeneration as evidenced by the lack of roof plate-associated structures in lizard regenerates (Fig. 1 and *SI Appendix*, Fig. S2). On examination of the ependymal tubes, we confirm that, as reported by Schnapp et al. (9) and Mchedlishvili et al. (7), the salamander ependymal tube expresses floor plate and roof plate markers in vivo, while we see that the lizard only expresses floor plate markers (Fig. 2 and *SI Appendix*, Fig. S3). However, in vitro, we found that salamander NSCs exhibit an exclusively default roof plate expression that is dependent on Shh signaling to ventralize patterning (Fig. 3 and *SI Appendix*, Fig. S5). This dependency is reminiscent of the fine balance of patterning molecules in the embryonic neural tube, and we also saw this in vivo where the ependymal tube dorsalizes in the absence of hedgehog signaling and floor plate structures, such as the cartilage rod, are lost (Figs. 4 and 5 and *SI Appendix*, Fig. S9), as shown earlier by Schnapp et al. (9), as well. This is in contrast to adult lizard ependymal tube and NSCs, which only express floor plate marker Shh in vitro and in vivo (Figs. 2 and 3 and *SI Appendix*, Figs. S3 and S5), correlating well with our previous studies (20, 25). (Of note, dorsoventral patterning of the embryonic lizard neural tube resembles that of the spinal cord and ependymal tube in salamander, a species that exhibits neoteny. However, this resemblance is limited to neuroanatomy, not regenerative strategy, as axolotls are amphibians, while lizards are amniotes.) Neither lizard ependyma nor NSCs dorsalize in response to abolished hedgehog signaling, although Shh-dependent cartilage tube formation is inhibited in vivo on treatment with cyclopamine (Figs. 4 and 5 and *SI Appendix*, Fig. S9). Indeed, SAG treatment in salamander tails mimics the natural rampant hedgehog signaling in lizard tails and results in ependymal tube dorsoventral patterning similar to that of the lizard regenerate, whereas cyclopamine treatment in lizards fails to abolish the patterning effects of unchecked Shh signaling and does not cause the regenerated tail to become more faithful to the original. This discrepancy in NSC activity clearly points to a difference in NSC behavior. Overall, the observations in vitro and in vivo are congruent with the structures and segmentation seen in the corresponding regenerates (14, 18, 19) and suggest that NSCs are responsible for inducing and patterning the lizard and salamander regenerate.

The observations that salamander NSCs exhibit a default roof plate identity in vitro while lizard NSCs default toward a floor plate identity raise the question of whether floor plate cells are being outcompeted in vitro. Taking a look at EdU staining in

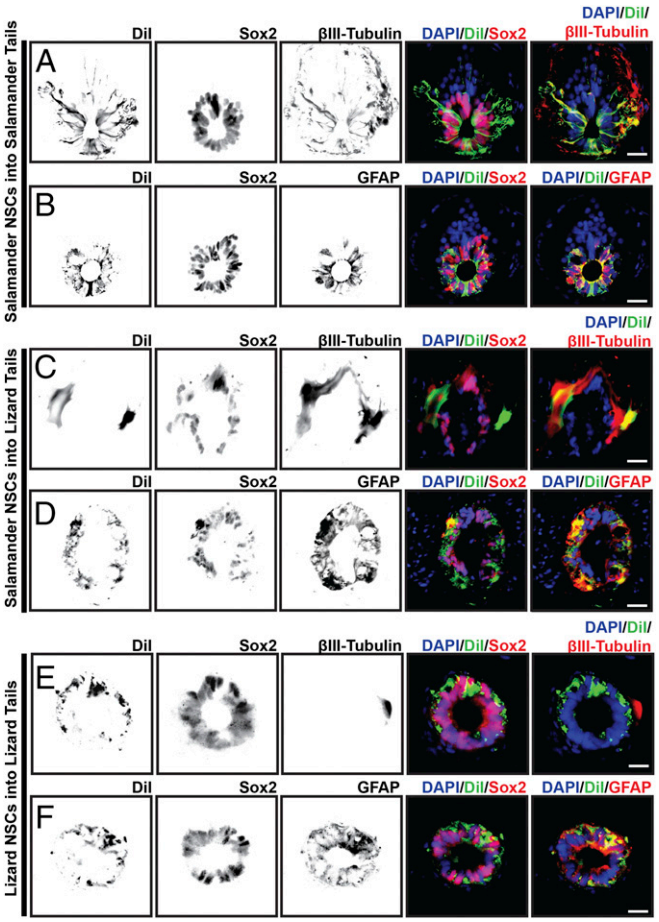

Fig. 10. Salamander (*A. mexicanum*) NSCs differentiate into neural lineages within the lizard (*L. lugubris*) tail microenvironment. Salamander and lizard neurospheres were cultured in vitro, DiI labeled, and injected into the spinal cord of an amputated salamander or lizard tail. Transverse sections of salamander (*A–D*) or lizard (*E* and *F*) regenerated ependymal tubes were stained for Sox2 and βIII-Tubulin (*A*, *C*, and *E*) or GFAP (*B*, *D*, and *F*). Salamander NSCs coexpressed DiI and βIII-Tubulin/GFAP when injected into either salamander or lizard tails. Lizard NSCs did not colocalize expression of DiI and βIII-Tubulin. Of note, lizard NSCs injected into salamander tails were nonviable. All regenerates are 4 wk postamputation/NSC injection. (Scale bar: 50 μm.)

vitro, we see evidence that this could potentially be the case: 42.8% of roof plate salamander NSCs are actively proliferating after 2 h of Edu incorporation, whereas only 7.9% of floor plate lizard NSCs are (*SI Appendix*, Fig. S6). In addition, in vivo EdU staining over a course of 8 wk shows that, while in general, the salamander is more proliferative (particularly at later time points, like 8 wk), it seems that roof plate-localized $Sox2^+$ cells are more proliferative than floor plate cells, especially in more proximal tail regions. However, the default roof plate identity could also be due to a lack of inductive signal for hedgehog expression that may be present ventrally within the salamander microenvironment but is lost when NSCs are isolated for in vitro culture. A full study on the proliferative capacities of these populations as they pertain to regeneration is beyond the scope of this study and will be addressed in future studies.

Interestingly, we found the differentiation potential of lizard NSCs to be limited compared with the salamander (7). Indeed, in vitro assays of differentiation and in vivo spinal cord transplantation show that lizard NSCs have limited ability to take on terminal neural fate (Figs. 7 and 8 and *SI Appendix*, Fig. S11). Other studies suggest that proliferating neural stem/progenitor is responsible for neurogenesis in regenerating lizard tails, but we observe that neurogenesis originates from the proximal spinal cord independent of resident NSCs (27, 28). This in part explains the lack of sensory and motor neuron regeneration in the spinal cords of newly formed lizard tail. Instead, sensory nerves of regenerated lizard tails arise from hypertrophied DRG proximal to the amputation site, similar to mammal peripheral nerve regeneration (14, 18, 19). The lack of lizard NSC neural differentiation capabilities represents a divergence from cognate NSCs capable of forming multiple neural lineages, even among non-regenerating mammals (29–36). A possible explanation for the restriction in lineage capabilities could be in the fact that the lizard tail spinal cord originates from a secondary neural tube formed from a mesodermal source, whereas the salamander tail spinal cord forms as part of the primary neural tube of ectodermal origin. Although lizard NSCs do not differentiate into neurons, they still reconstitute the regenerating ependymal tube similar to salamander NSCs (Fig. 10 *E* and *F* and *SI Appendix*, Fig. S13). However, lizard NSCs contribute to a strongly ventralizing environment as evidenced by salamander neurosphere ventralization within the lizard tail (Fig. 9*A* and *SI Appendix*, Fig. S15). Only with hedgehog signaling blockade, roof plate expression is maintained, and spatially segregated patterning is observed within the regenerated lizard tail environment, which points to a possible pathway to restore appropriate patterning in the regenerate.

These observations and findings beg the question: what is the identity of lizard NSCs? Curiously, it is known that neural differentiation from stem cells (in particular, oligodendrocyte lineage) is dependent on Shh expression in various species, including mice and zebrafish (37, 38). At the same time, Shh has been shown to inhibit neural differentiation while up-regulating proliferation in postmitotic precursor neural cells at late fetal stages (of note, Shh overexpression is also thought to be responsible for some primitive neuroectodermal tumors) (39, 40). This is further complicated by the finding that Shh signaling requires up-regulation of Sulfatase1 in a temporal fashion to effectively induce neural progenitors in zebrafish (41). We posit that lizard NSCs are in fact "cognate" NSCs that lack expression of a regulating gene for Shh expression, which leads to suppression of differentiation and the phenotypically nonidentical patterns of tail regeneration observed. This partly stems from observations that neotenic salamander NSCs are able to differentiate into neurons even after being ventralized by the lizard microenvironment, indicating that the "defect" is likely intrinsic to the lizard NSCs (Fig. 10 and *SI Appendix*, Fig. S15). In addition, the fact that lizard NSCs in original adult tails are solely floor plate while embryonic tails express all domains hints that perhaps expression of a gene may be lost in adulthood (of note, axolotol NSCs have been found to express Nogo-A and Nogo receptor during regeneration, which could potentially also be genes of interest) (42) (Fig. 2 and *SI Appendix*, Fig. S3). Future studies will, therefore, probe the identities of embryonic lizard NSCs vs. adult lizard NSCs. However, for now, we recognize that these cells are not true NSCs, and we find the term "$Sox2^+$ ependymal progenitor cells" to be more fitting for this population until additional evidence proves otherwise.

In studying lizards vs. salamanders, we seek to discover the key pathways that delineate the species in terms of regeneration potential to shed light on pathways lost in mammalian healing. We have shown here that $Sox2^+$ NSCs are in part responsible for the lack of patterning observed in the lizard regenerate. We recognize that an inherent limitation in our study was our inability to target only NSC populations in vivo to knock down Shh expression in a localized manner to really probe the sole contribution of the NSCs to patterning. Unfortunately, given the reproductive cycle of the lizard, transgenic approaches are not yet available to us. We will look toward developing techniques to implant NSCs/neurospheres into the regenerating spinal cord to overcome these limitations, and future studies will now focus on modulating lizard NSC behavior and probing their identity to effect improved regeneration.

Materials and Methods

All reagents/chemicals were purchased from Sigma-Aldrich unless otherwise specified.

Salamander and Lizards. All experiments were carried out with the salamander *A. mexicanum* and repeated with two lizard species, the mourning gecko *Lepidodactylus lugubris* and the green anole *Anolis carolinensis*. The choice to include the two lizard species is twofold. First, the gekkonid *L. lugubris* and the iguanid *A. carolinensis* represent the two main lizard families used in regeneration research, and their simultaneous inclusion and the fact that we observed nearly identical behaviors in the cell and tissue types tested allowed for higher confidence that the conclusions made here apply to regenerative lizards as a broad group. Second, distinctive traits exhibited by each species facilitate specific experimental methods. For example, the calcified cartilage tubes of regenerated *A. carolinensis* tails facilitated spinal cord implantation studies, while the high productivity of the parthenogenetic *L. lugubris* allowed for the generation of enough source material for generating NSCs used in injection studies. All lizard and salamander studies were performed according to the guidelines of the Institutional Animal Care and Use Committee at the University of Pittsburgh (protocol nos. 15114947, 16128889, and 18011476). In this study, we used adult lizard and salamander tail regenerates at 2, 4, and 8 wk post-amputation. Lizards and salamanders follow similar time courses in their tail regenerations (*SI Appendix*, Fig. S1), and comparing time-matched samples limited bias during interspecies comparisons.

Isolation of NSCs and Generation of Neurospheres. To generate lizard and salamander neurospheres, spinal cords were isolated from original lizard and salamander tails, dissociated, and expanded as previously reported (20, 25). Briefly, the spinal cords were cut into small pieces, digested, and filtered; myelin was carefully aspirated, and lastly, the pellet was resuspended in neurosphere medium and plated at a density of ~40,000 cells per well. After 4 wk, primary neurospheres were utilized for additional experiments. *SI Appendix, SI Materials and Methods* has additional information.

Injection of Neurospheres. After 4 wk in culture, neurospheres were collected, trypsinized, and resuspended in PBS (Gibco). To track the cells in vivo, they were labeled with DiI labeling with Vibrant CM solution (Invitrogen) according to the manufacturer's instructions and resuspended at a density of 10,000 cells per 1 μL for injection into the ependymal tube. Recipient animals were treated with a 50-μL i.p. injection of Tacrolimus (Selleckchem) every 48 h at a concentration of 20 μg/mL; 2–3 μL of cell suspension containing 10,000 DiI-labeled NSCs per 1 μL was injected into the spinal cord with a 36-gauge needle, and the animals were allowed to return immediately to their enclosure and resume normal activities. *SI Appendix, SI Materials and Methods* has additional information.

Injection Regimen. Salamanders were anesthetized before i.p. injection by exposure to Benzocaine (RND Center INC.) at a concentration of 0.5 mg/L and allowed to recover from anesthesia in fresh water before returning to their enclosure. Lizards were not anesthetized before injection. The injection regimen for treatment groups consisted of i.p. injections every other day for 3 wk of SAG (Selleckchem), Cyclopamine (LC Laboratories), or vehicle control as follows: SAG group, 50–100 μL of SAG at a concentration of 800 μg/mL (43); cyclopamine group, 50–100 μL of cyclopamine at a concentration of 500 μg/mL; vehicle control, 100 μL of 2% DMSO (Life Technologies) for molecular biology diluted in PBS (Gibco).

Differentiation Assay. Neurospheres were differentiated by plating onto glass slides coated with laminin/poly-L-lysine and culturing in neurosphere medium without basic fibroblast growth factor and heparin (standard differentiation medium). An oligodendrocyte-favoring protocol was also used, which involved culturing in standard differentiation medium with supplementation of SAG (50 ng/mL) and PDGF (25 ng/mL; Peprotech). After 2 wk of culture, samples were fixed in 4% paraformaldehyde and processed for immunohistochemistry (IHC).

Tail Sample Collection. Samples were collected 2, 4, or 8 wk after original tail amputation. Salamanders were anesthetized by exposure to Benzocaine (RND Center INC.) at a concentration of 1 mg/L. Regenerated tails were amputated with a number 22 scalpel blade. The animals were allowed to recover from anesthesia in fresh water before returning to their enclosure and normal activity. Lizard tails were collected by amputation with a number 22 scalpel blade followed by immediate return to enclosure and normal activity.

IHC. Lizard and salamander tissue samples were analyzed by IHC as previously described (44). *SI Appendix*, Table S2 has IHC antibody specifics. All IHC images of sagittal sections are presented dorsal toward the top, ventral toward the bottom, distal toward the right, and proximal toward the left. Transverse sections are presented with dorsal on top and ventral on bottom.

Statistical Analysis. Statistical analysis was performed using Prism 7 with one- or two-way ANOVA with pairwise Tukey's multiple comparison test for data with multiple groups. A P value of <0.05 was deemed to be statistically significant. All values and graphs are shown as mean ± SD.

ACKNOWLEDGMENTS. We thank Dr. Wei Wenzhong for his help in validating real time RT-PCR in lizard samples. We also thank Danielle Danucalov, Christian DeMoya, Nicole Eng, Sara Kenes, Ashley Martier, Beatrice Milnes, and Sean Tighe for their help in maintaining lizard and salamander colonies. We acknowledge funding from NIH Grant R01GM115444.

1. Bely AE (2010) Evolutionary loss of animal regeneration: Pattern and process. *Integr Comp Biol* 50:515–527.
2. Bely AE, Nyberg KG (2010) Evolution of animal regeneration: Re-emergence of a field. *Trends Ecol Evol* 25:161–170.
3. Londono R, Sun AX, Tuan RS, Lozito TP (2018) Tissue repair and epimorphic regeneration: An overview. *Curr Pathobiol Rep* 6:61–69.
4. Sugiura T, Wang H, Barsacchi R, Simon A, Tanaka EM (2016) MARCKS-like protein is an initiating molecule in axolotl appendage regeneration. *Nature* 531:237–240.
5. Hutchison C, Pilote M, Roy S (2007) The axolotl limb: A model for bone development, regeneration and fracture healing. *Bone* 40:45–56.
6. McCusker C, Gardiner DM (2011) The axolotl model for regeneration and aging research: A mini-review. *Gerontology* 57:565–571.
7. McHedlishvili L, et al. (2012) Reconstitution of the central and peripheral nervous system during salamander tail regeneration. *Proc Natl Acad Sci USA* 109:E2258–E2266.
8. Satoh A, Makanae A, Nishimoto Y, Mitogawa K (2016) FGF and BMP derived from dorsal root ganglia regulate blastema induction in limb regeneration in Ambystoma mexicanum. *Dev Biol* 417:114–125.
9. Schnapp E, Kragl M, Rubin L, Tanaka EM (2005) Hedgehog signaling controls dorsoventral patterning, blastema cell proliferation and cartilage induction during axolotl tail regeneration. *Development* 132:3243–3253.
10. Voss SR, Epperlein HH, Tanaka EM (2009) Ambystoma mexicanum, the axolotl: A versatile amphibian model for regeneration, development, and evolution studies. *Cold Spring Harb Protoc* 2009:pdb.emo128.
11. Nacu E, Gromberg E, Oliveira CR, Drechsel D, Tanaka EM (2016) FGF8 and SHH substitute for anterior-posterior tissue interactions to induce limb regeneration. *Nature* 533:407–410.
12. Kragl M, et al. (2009) Cells keep a memory of their tissue origin during axolotl limb regeneration. *Nature* 460:60–65.
13. Sandoval-Guzmán T, et al. (2014) Fundamental differences in dedifferentiation and stem cell recruitment during skeletal muscle regeneration in two salamander species. *Cell Stem Cell* 14:174–187.
14. Alibardi L (2010) Morphological and cellular aspects of tail and limb regeneration in lizards. A model system with implications for tissue regeneration in mammals. *Adv Anat Embryol Cell Biol* 207:1–109.
15. Lozito TP, Tuan RS (2017) Lizard tail regeneration as an instructive model of enhanced healing capabilities in an adult amniote. *Connect Tissue Res* 58:145–154.
16. McLean KE, Vickaryous MK (2011) A novel amniote model of epimorphic regeneration: The leopard gecko, Eublepharis macularius. *BMC Dev Biol* 11:50.
17. Ritzman TB, et al. (2012) The gross anatomy of the original and regenerated tail in the green anole (Anolis carolinensis). *Anat Rec (Hoboken)* 295:1596–1608.
18. Fisher RE, et al. (2012) A histological comparison of the original and regenerated tail in the green anole, *Anolis carolinensis*. *Anat Rec (Hoboken)* 295:1609–1619.
19. Bellairs A, Bryant SV (1985) Autotomy and regeneration in reptiles. *Biology of the Reptilia: Development B* (John Wiley & Sons, New York), Vol 15, pp 301–410.
20. Lozito TP, Tuan RS (2016) Lizard tail skeletal regeneration combines aspects of fracture healing and blastema-based regeneration. *Development* 143:2946–2957.
21. Dessaud E, McMahon AP, Briscoe J (2008) Pattern formation in the vertebrate neural tube: A sonic hedgehog morphogen-regulated transcriptional network. *Development* 135:2489–2503.
22. Briscoe J, Small S (2015) Morphogen rules: Design principles of gradient-mediated embryo patterning. *Development* 142:3996–4009.
23. McHedlishvili L, Epperlein HH, Telzerow A, Tanaka EM (2007) A clonal analysis of neural progenitors during axolotl spinal cord regeneration reveals evidence for both spatially restricted and multipotent progenitors. *Development* 134:2083–2093.
24. Albors AR, et al. (2015) Planar cell polarity-mediated induction of neural stem cell expansion during axolotl spinal cord regeneration. *Elife* 4:e10230.
25. Lozito TP, Tuan RS (2015) Lizard tail regeneration: Regulation of two distinct cartilage regions by Indian hedgehog. *Dev Biol* 399:249–262.
26. Maden M, Manwell LA, Ormerod BK (2013) Proliferation zones in the axolotl brain and regeneration of the telencephalon. *Neural Dev* 8:1.
27. Zhou Y, et al. (2013) Early neurogenesis during caudal spinal cord regeneration in adult Gekko japonicus. *J Mol Histol* 44:291–297.
28. Gilbert EAB, Vickaryous MK (2018) Neural stem/progenitor cells are activated during tail regeneration in the leopard gecko (Eublepharis macularius). *J Comp Neurol* 526: 285–309.
29. Stemple DL, Anderson DJ (1992) Isolation of a stem cell for neurons and glia from the mammalian neural crest. *Cell* 71:973–985.
30. Reynolds BA, Weiss S (1992) Generation of neurons and astrocytes from isolated cells of the adult mammalian central nervous system. *Science* 255:1707–1710.
31. Rao MS (1999) Multipotent and restricted precursors in the central nervous system. *Anat Rec* 257:137–148.
32. Reynolds BA, Tetzlaff W, Weiss S (1992) A multipotent EGF-responsive striatal embryonic progenitor cell produces neurons and astrocytes. *J Neurosci* 12:4565–4574.
33. Cattaneo E, McKay R (1990) Proliferation and differentiation of neuronal stem cells regulated by nerve growth factor. *Nature* 347:762–765.
34. Temple S (1989) Division and differentiation of isolated CNS blast cells in microculture. *Nature* 340:471–473.
35. Temple S (2001) The development of neural stem cells. *Nature* 414:112–117.
36. Gage FH (2000) Mammalian neural stem cells. *Science* 287:1433–1438.
37. Shitasako S, et al. (2017) Wnt and Shh signals regulate neural stem cell proliferation and differentiation in the optic tectum of adult zebrafish. *Dev Neurobiol* 77: 1206–1220.
38. Rowitch DH, et al. (1999) Sonic hedgehog regulates proliferation and inhibits differentiation of CNS precursor cells. *J Neurosci* 19:8954–8965.
39. Palma V, et al. (2005) Sonic hedgehog controls stem cell behavior in the postnatal and adult brain. *Development* 132:335–344.
40. Marino S (2005) Medulloblastoma: Developmental mechanisms out of control. *Trends Mol Med* 11:17–22.
41. Al Oustah A, et al. (2014) Dynamics of sonic hedgehog signaling in the ventral spinal cord are controlled by intrinsic changes in source cells requiring sulfatase 1. *Development* 141:1392–1403.
42. Hui SP, Monaghan JR, Voss SR, Ghosh S (2013) Expression pattern of Nogo-A, MAG, and NgR in regenerating urodele spinal cord. *Dev Dyn* 242:847–860.
43. Heine VM, et al. (2011) Preterm birth: A small-molecule smoothened agonist prevents glucocorticoid-induced neonatal cerebellar injury. *Sci Transl Med* 3:105ra104.
44. Londono R, Wenzhong W, Wang B, Tuan RS, Lozito TP (2017) Cartilage and muscle cell fate and origins during lizard tail regeneration. *Front Bioeng Biotechnol* 5:70.